AD-A090 337 SHEFFIELD UNIV (ENGLAND) DEPT OF CHEMICAL ENGINEERIN--ETC F/G 21/5
A THREE-DIMENSIONAL MODEL OF SPRAY EVAPORATION IN GAS TURBINE C--ETC(U)
APR 80 W H AYERS AFOSR-80-0174
UNCLASSIFIED HIC-343 AFOSR-TR-80-0928 NL

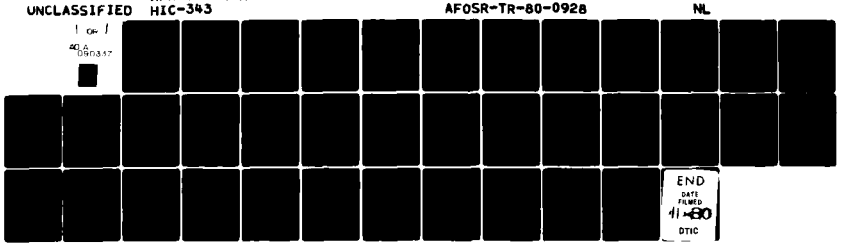

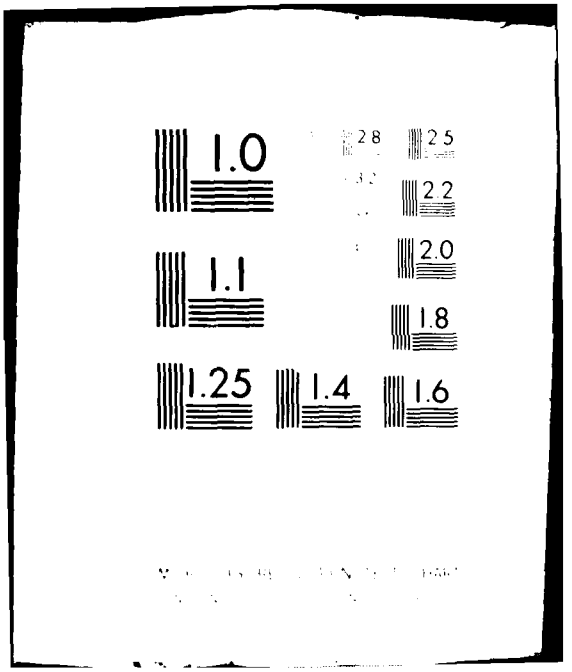
1.0
2.8
2.5
2.2
2.0
1.1
1.8
1.25
1.4
1.6

A Three-Dimensional Model of Spray Evaporation in Gas Turbine Combustors.

W. H. Ayers

Apr[illegible]80.

UNCLASSIFIED

SECURITY CLASSIFICATION OF THIS PAGE (When Data Entered)

REPORT DOCUMENTATION PAGE	READ INSTRUCTIONS BEFORE COMPLETING FORM
1. REPORT NUMBER AFOSR-TR-80-0928	2. GOVT ACCESSION NO. AD-A090337
	3. RECIPIENT'S CATALOG NUMBER
4. TITLE (and Subtitle) A THREE DIMENSIONAL MODEL OF SPRAY EVAPORATION IN GAS TURBINE COMBUSTORS	5. TYPE OF REPORT & PERIOD COVERED Interim
	6. PERFORMING ORG. REPORT NUMBER HIC 343
7. AUTHOR(s) W H AYERS	8. CONTRACT OR GRANT NUMBER(s) AFOSR-80-0174
9. PERFORMING ORGANIZATION NAME AND ADDRESS UNIVERSITY OF SHEFFIELD MAPIN STREET SHEFFIELD, S1 3JD	10. PROGRAM ELEMENT, PROJECT, TASK AREA & WORK UNIT NUMBERS 2308/A2 61102F
11. CONTROLLING OFFICE NAME AND ADDRESS AIR FORCE OFFICE OF SCIENTIFIC RESEARCH/NM BUILDING 410 BOLLING AFB, DC 20332	12. REPORT DATE April 1980 13. NUMBER OF PAGES 33
14. MONITORING AGENCY NAME & ADDRESS(if different from Controlling Office)	15. SECURITY CLASS. (of this report) UNCLASSIFIED 15a. DECLASSIFICATION DOWNGRADING SCHEDULE

16. DISTRIBUTION STATEMENT (of this Report)

Approved for public release; distribution unlimited.

17. DISTRIBUTION STATEMENT (of the abstract entered in Block 20, if different from Report)

18. SUPPLEMENTARY NOTES

19. KEY WORDS (Continue on reverse side if necessary and identify by block number)

SPRAY
COMBUSTION
DROPLETS
THREE DIMENSIONAL COMPUTATIONS
MATHEMATICAL MODELING
GAS TURBINE COMBUSTION
TWO PHASE FLOW

20. ABSTRACT (Continue on reverse side if necessary and identify by block number)

The result of this study is a computer program which can calculate the trajectory of a droplet or particle in three dimensions in a three dimensional flow field. Droplets are injected into a computer predicted flow field in a gas turbine combustor can with initial conditions corresponding to the point of sheet break up of fuel leaving the atomizer being modeled. The fundamental equations of motion are solved numerically for each droplet size in a statistical distribution representing the whole spray. The angular position of the point of injection is also varied. The rate of fuel evaporation in each cell of the

DD FORM 1 JAN 73 1473

UNCLASSIFIED

SECURITY CLASSIFICATION OF THIS PAGE (When Data Entered)

Summary

The result of this study is a computer programme which can calculate the trajectory ofadroplet or particle in three dimensions in a three dimensional flow field.

Droplets are injected into a computer predicted flow field in a gas turbine combustor can with initial conditions corresponding to the point of sheet break-up of fuel leaving the atomiser being modelled. The fundamental equations of motion are solved numerically for each droplet size in a statistical distribution representing the whole spray. The angular position of the point of injection is also varied.

The rate of fuel evaporation in each cell of the finite difference grid is then calculated so that this can be used for improved flow field calculations. Droplet trajectories are also presented graphically to give information on the three-dimensional nature of the spray.

Contents.

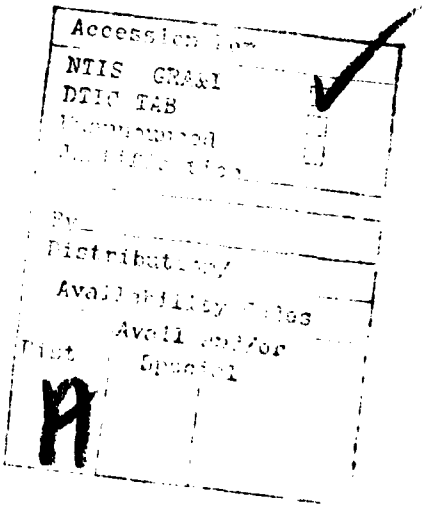

Notation.

C_b	Evaporation constant
C_D	Drag coefficient
c_p	Specific heat capacity at constant pressure
D_p	Droplet or particle diameter
$\bar{D}$	Rosin-Rammler mean diameter
L	Latent heat of evaporation
m	Mass
$\dot{m}$	Mass flowrate
n	Rosin-Rammler spread parameter
Nu	Nusselt number
Pr	Prandtl number
Re	Reynolds number
t	Time
T	Temperature
$\vec{u}$	Resultant velocity vector
u, v, w	velocity components in axial, radial and tangential directions.
$\dot{u}$, $\dot{v}$, $\dot{w}$	time derivatives of u, v and w
x, y, z	distance in axial, radial and angular directions.
$\dot{x}$, $\dot{y}$, $\dot{z}$	time derivatives of x, y and z.

ρ	Density
μ	Viscosity
λ	Thermal conductivity

Subscripts:

o	Initial
∞	Flow field
g	Gas
ℓ	Liquid
p	Particle or droplet

Introduction.

The availability of large general purpose digital computers has enabled numerical techniques to be applied to complex physical phenomena. In the field of Combustion Research, mathematical modelling can be used to predict the behaviour of all kinds of combustion processes and can give information on the chemical and physical processes taking place (Ref. 1). As a design tool, mathematical modelling can assist in providing a less empirical approach to the problems of combustor design, a field of increasing importance as a result of the present interest in improved fuel efficiency and reduction of pollutant emissions.

The object of this study is to produce a general algorithm to calculate the trajectory of a particle in a gas flow in three dimensions. The equations of motion and trajectory are solved numerically, as an analytical solution is not practicable in three dimensions with the coordinate system used.

The algorithm is then applied to the specific case of evaporating fuel droplets in a gas turbine combustor, in order to model mathematically the spray evaporation taking place and to provide information on the trajectories and behaviour of individual droplets and size groups with varying initial conditions.

In order to model the evaporating droplets, equations representing droplet heating up and evaporation must be included in the trajectory algorithm.

The computer predicted gas flow field for a Lycoming combustor, used in the study, was produced at Sheffield (ref. 2), and defines the geometry of the finite difference grid into which droplets are injected.

Work in this field has already produced droplet trajectories in two dimensions (Ref. 5).

Having obtained trajectories of individual droplets, the model is extended to an entire spray by calculating the trajectories of a range of droplet sizes and initial conditions. The trajectories are presented graphically to yield information on the behaviour of individual droplets within the spray.

The rate of fuel evaporation in each grid cell can also be calculated for the fuel spray. This information can then be used in the original flow field calculations, replacing the time consuming method currently used, i.e. representing each droplet size range as a chemical species and solving the resulting elliptic equations.

Theory.

Because of the cylindrical nature of combustion chambers and the gas flows involved, a cylindrical polar coordinate system is used to describe the location of the particle or droplet, where x is the axial distance from the datum, y is the radial position, and z (radians) is the angular position. Velocities are measured in the axial (u), radial (v) and tangential (w) directions.

The equations of motion of a particle, neglecting all forces except drag, in component form are:

$$\dot{u}_p = -F\left(u_p - u_\infty\right) \tag{1}$$

$$\dot{v}_p = \frac{w_p^2}{y_p} - F\left(v_p - v_\infty\right) \tag{2}$$

$$\dot{w}_p = -\frac{v_p\, w_p}{y_p} - F\left(w_p - w_\infty\right) \tag{3}$$

where u_p, v_p, w_p are the absolute particle velocities in the axial, radial and tangential directions respectively, and $u_\infty, v_\infty, w_\infty$ are the corresponding gas velocities.

For the general case, F is given by:

$$F = \left(\frac{18\,\mu_g}{\rho_p\, D_p^2}\right) \cdot \left(\frac{C_D\, Re}{24}\right) \tag{4}$$

where D_p is the particle diameter, Re is the relative Reynold's number, defined as:

$$Re = \frac{D_p \rho_g}{\mu_g} \cdot \left| \vec{u}_p - \vec{u}_\infty \right| \qquad (5)$$

where $\vec{u}_p$ and $\vec{u}_\infty$ are the resultant velocities of the particle and gas stream respectively.

The drag coefficient, C_D, is given by the following equations (Ref. 3) :

$$C_D = 27\, Re^{-0.84} \qquad 0 < Re \leq 80 \qquad (6)$$

$$C_D = 0.271\, Re^{0.217} \qquad 80 < Re \leq 10^4 \qquad (7)$$

$$C_D = 2 \qquad 10^4 < Re \qquad (8)$$

If Stoke's regime prevails and there is uniform gas flow (i.e. $u_\infty, v_\infty, w_\infty$ are constant), then the axial component can be solved analytically.

Under Stoke's regime, the term $\left(\frac{C_D\, Re}{24}\right)$ is approximated to unity.

Assuming D_p remains constant, the term $\left(\frac{18\,\mu_g}{\rho_l\, D_p^2}\right)$ becomes constant, whereupon equation (1) is integrable.

In a Cartesian coordinate system, the equations of motion for all three components would have the form of equation (1), thus permitting an analytical solution for obtaining the droplet or particle trajectories. However, in the rectangular polar coordinate system used, the interdependence in the expressions for the radial and tangential components prevents an analytical solution being found.

For the rectangular polar coordinate system, the equations of trajectory are:

$$\dot{x}_p = u_p \qquad (9)$$

$$\dot{y}_p = v_p \qquad (10)$$

$$\dot{z}_p = \frac{w_p}{y_p} \qquad (11)$$

Equations (1) to (11) describe the trajectory of a particle in a gas stream. For an evaporating droplet, D_p is not constant, and the rate of change of droplet diameter with time is required. For forced convection this is given by:

$$\frac{d D_p}{dt} = - \frac{C_b}{2 D_p} \left(1 + 0.23 R_e^{1/2} \right) \qquad (12)$$

where C_b is the evaporation constant. This is dependant on the properties of the fuel as well as the surrounding gases, and is given by Wise and Agoston as (Ref. 4) :

$$C_b = \frac{8 \lambda_g}{\rho_l c_{pg}} \ln \left(1 + \frac{c_{pg}}{L} \left(T_\infty - T_l \right) \right) \qquad (13)$$

If $\left(1 + 0.23 R_e^{1/2}\right)$ can be assumed constant, then equation (12) can be integrated to give:

$$D_p^2 = D_{po}^2 - C_b \left(1 + 0.23 Re^{1/2}\right)(t - t_o) \qquad (14)$$

representing the droplet diameter D_p at time t, where D_{po} is the droplet diameter at time t_o.

To allow for droplets "heating up" after entry into the hot gas stream it has been assumed that droplets do not begin to evaporate until they reach their boiling point. The rate of change of temperature with time is given by:

$$\frac{dT_p}{dt} = \frac{6\,Nu\,\lambda_g}{\rho_l\,D_p^2\,C_{p_l}} \cdot (T_\infty - T_p) \qquad (15)$$

where T_p is the droplet temperature. Assuming $\left(\frac{6\,Nu\,\lambda_g}{\rho_l\,D_p^2\,C_{p_l}}\right)$ is constant, on integration this gives:

$$T_p = T_\infty - (T_\infty - T_{po})\,exp\left(\frac{-6\,Nu\,\lambda_g}{\rho_l\,D_p^2\,C_{p_l}}\cdot(t-t_o)\right) \qquad (16)$$

where T_{po} is the drop temperature at time t_o.

Equation (14) is suppressed until the droplet temperature, reaches the boiling point of the liquid. The Nusselt number, Nu is given by:

$$Nu = 2 + 0.6\,Re^{1/2}\,Pr^{1/3} \qquad (17)$$

where the Prandtl number, Pr is given by:

$$Pr = \frac{C_{p_g}\,\mu_g}{\lambda_g} \qquad (18)$$

The above solutions are, of course, valid only when $(t-t_o)$ is taken to be sufficiently small.

Application.

Equations (1) to (18) above describe the motion of an evaporating droplet in three dimensions in a gas stream. Numerical integration can now be used to calculate the droplet trajectory in the given gas flow field.

For the purposes of this investigation a computer predicted flow field in a gas turbine combustor was used. This has been calculated for a Lycoming combustor using a numerical prediction algorithm to model the physical and chemical processes taking place (Ref. 2).

The geometry of the Lycoming combustor can, which was designed as a research combustor, is shown in Fig. 1. Air enters via a swirler which produces a finite swirl velocity. The fuel spray is introduced at a point near the centre line in front of a baffle and is of hollow cone type. Primary, secondary and dilution air streams are introduced by three sets of injection holes, each consisting of six equally spaced circular orifices around the periphery of the combustor can. This is responsible for the three-dimensional nature of the problem.

For the computer model, the combustor can is represented by a single 60° sector containing one set of air injection holes to represent the six identical segments. This is then subdivided into a further 7 sectors. In the axial direction the length of the combustor is divided into 27 sections, and radially into 18 sections, giving a total of 3402 elements in the finite difference grid. The grid is shown in Fig. 2.

The elements are labelled (I,J,K) in the x,y and z directions. Note that in the angular direction elements with K between 2 and 6 inclusive occupy 10° sectors whereas the K=1 and K=7 elements occupy a sector of 5° . In fact the two 5°

sectors are adjacent and can be considered as one 10^{o} sector, but due to the positioning of the grid and in order to simplify calculations they are considered as two separate half sectors.

For the purposes of this investigation the flow parameters used (which are the three components of velocity, temperature and density) are defined for each grid element and are assumed to be valid throughout this control volume. The complex flow throughout the combustor can thus be represented by the finite difference grid.

The flow data is obtained from the output of the combustor model described in Ref. 2. The same grid geometry is used in the latter but the gas velocities are defined for a staggered grid. This is demonstrated by Fig. 3(a) which shows that the u , v and w velocity control volumes do not coincide with those for temperature, pressure etc. In order to considerably simplify the representation of velocity data the u, v, w velocity control volumes have been redefined to coincide with the nominal control volumes by averaging adjacent velocity values, an example being shown in Fig. 3(b).

Since the first set of air injection holes occurs at the primary air inlet it might be expected that the gas flow field would be essentially two dimensional upstream from this point. It is on this assumption that the two dimensional model of Ref. 5 is justified. To investigate the validity of this assumption a statistical analysis of u-, v- and w-velocity, temperature and density data was made. For each value of I and each of three J values, the set of data for all K values was averaged and a sample standard deviation calculated.

Sample standard deviation, s, is given by:

$$s = \left(\frac{\sum_{i=1}^{i=n} (x_i - \bar{x})^2}{n-1} \right)^{1/2} \qquad (19)$$

where $x_1, x_2 \ldots\ldots x_n$ are the values of the data, $\bar{x}$ is the mean of the data and n is the number of data points. Since we are interested in the amount of angular variation as a proportion of the mean of the values rather than the absolute variation, the sample standard deviation is expressed as a percentage of the mean. Hence:

$$\text{Sample Standard Deviation (Percent)} = \frac{100}{\bar{x}} \left(\frac{\sum_{i=1}^{i=n} (x_i - \bar{x})^2}{n-1} \right)^{1/2} \qquad (20)$$

The results of this analysis are shown in Figs. 4(a) to 4(e), and are discussed below.

A vector plot of the velocity distribution is also given in Figs. 5(a) and 5(b). It can be clearly seen that there is a recirculation zone in front of the baffle, and that the flow in the region of the air injection holes is dominated by the inward flow of air. The flow cross-section of Fig. 5(b) at the point of primary air inlet clearly shows how the three-dimensional nature of the flow field is brought about by the disturbance introduced by the air injection.

Once the u-, v-, w-velocity, temperature and density data is stored as a 27 x 18 x 7 array, the fundamental equations of motion (equations (1), (2) and (3)) can be solved numerically by assuming that the gas velocity, temperature and density remain constant throughout each cell.

These three simultaneous differential equations are solved by using the fourth order Runge-Kutta method. The time step length is calculated to give approximately the same number of time steps while the droplet is in each cell. After each time step the equations of trajectory (equations (9), (10) and (11)) are used in finite difference form to calculate the new values of x, y and z as follows:

$$x_n = x_{n-1} + \frac{1}{2} \cdot t_{step} \left(u_n + u_{n-1} \right) \qquad (21)$$

$$y_n = y_{n+1} + \frac{1}{2} \cdot t_{step} \left(v_n + v_{n-1} \right) \qquad (22)$$

$$z_n = z_{n-1} + \frac{1}{2} \cdot t_{step} \left(\frac{w_n}{y_n} + \frac{w_{n-1}}{y_{n-1}} \right) \qquad (23)$$

In addition, for an evaporating droplet, either equation (14) or (16) is used, depending on whether the droplet has reached its boiling point, to calculate droplet diameter or temperature. Any auxiliary equations with terms containing u, v, w, x, y or z or D_p are also calculated after each time step.

A check is also made, after each time step, to establish whether the particle or droplet has passed through the boundary of the volume cell. If this proves to be the case the new cell is found and new values for the constants for the cell are obtained. Also, D_{p_0} of equation (14) and T_{p_0} of equation (16) and the corresponding t_0 are reset. A new time step length is calculated to maintain an approximately constant number of time steps in each cell. A check is also made for the following specific cases:

1) Droplet passes into an adjacent 60° sector.
   In this case the z value of the droplet is adjusted to bring it to the corresponding position in the original sector, i.e. 60° is subtracted from its z value. The actual angular position is retained for output.

2) Droplet passes through centre-line.
   Although there would seem to be a very small chance of this occurring a provision is incorporated for the droplet to be reflected from the centre-line if the radial distance, y, should become less than zero.

3) Droplet hits a wall.
   Since the original velocity data is not valid for cells for which J is greater than 17, a droplet is said to have hit the combustor wall if it enters a cell for which J is equal to 18.

4) Droplet passes through the exit of the combustion chamber. If a droplet or particle survives to pass through a cell for which I = 27 it is reported as having left the combustion chamber.

5) Droplet evaporates.
If the diameter of an evaporating droplet falls to less than $(10^{-m})^{\frac{1}{i}}$ metres (approximately 3 microns) it is reported as having evaporated. In practice, droplets vanish almost immediately as D_p becomes very small, and droplets smaller than this behave erratically unless the time step length is reduced greatly. This test is made with each time step.

6) Droplet remains in combustion chamber after 500 time steps. The iteration is halted if more than 500 time steps are required in order to prevent an excessive use of computer time.

Any of conditions 3) to 6) above will terminate the iteration loop, otherwise the next time step is calculated.

When a droplet is evaporating the amount of fuel evaporated per unit time in each cell is calculated as it leaves the cell, given by:

$$\dot{m}_{evap} = \left(\frac{D_{out}^3 - D_{in}^3}{D_{initial}^3} \right) \cdot \dot{m}_{fuel} \qquad (24)$$

where D_{in} = droplet diameter on entry into cell
D_{out} = droplet diameter on exit from cell
$D_{initial}$ = droplet diameter on start of trajectory
$\dot{m}_{fuel}$ = total mass flowrate of fuel represented by the droplet, e.g. the mass flowrate of fuel in the size range being represented by a single droplet.

If the droplet hits a wall as in 3) above, the remaining fuel contained in the droplet is "evaporated" into the cell adjacent to the wall, representing droplets adhering to the wall of the combustion chamber. It would be possible to extend the model to include droplets rebounding off the wall, shattering etc.

To extend the model to predict the behaviour of a whole spray, a statistical size distribution is used to represent the spray as a number of size ranges, each represented in turn by a single droplet diameter, the mean of the size range.

It is assumed that after sheet break-up, the fuel spray leaving the atomiser obeys a Rosin-Rammler size distribution. In this model, the mass fraction of fuel having a droplet diameter greater than D is given as:

$$m_D = \exp\left\{-\left(\frac{D}{\bar{D}}\right)^n\right\} \qquad (25)$$

where $\bar{D}$ is the Rosin-Rammler mean diameter and n is the spread parameter. For this study a value 50 microns was chosen for $\bar{D}$ and the spread parameter is taken as 2. The mass fraction of fuel in a given size range is found by subtraction:

$$m_{range} = \left| \exp\left\{-\left(\frac{D_1}{\bar{D}}\right)^n\right\} - \exp\left\{-\left(\frac{D_2}{\bar{D}}\right)^n\right\} \right| \qquad (26)$$

where the size range lies between D_1 and D_2 .

The size ranges are chosen to be of equal length and cover droplet diameters from zero to a diameter below which 99% of the mass of fuel falls. A total of 20 size ranges was chosen to adequately model the complete spray.

Single droplets with diameters equal to the mean of each size range are injected into the gas flow field with initial x and y coordinates corresponding to the point of sheet break-up of the spray. In addition, for each size range, droplets are injected from six different angular locations differing by 10^{o}. Consequently the trajectories of a total of 120 fuel droplets are calculated.

The atomiser characteristics are specified by spray cone angle, velocity, distance from nozzle to sheet break-up, and the Rosin-Rammler mean and spread parameter. From this and general physical data the entire spray cone is constructed.

The amount of fuel evaporated in each cell is summed for the whole spray. The mass flowrate of fuel represented by each droplet trajectory is:

$$\dot{m}_{fuel} = \frac{m_{range}}{6} \cdot \dot{m}_{total} \qquad (27)$$

where m_{range} is defined in equation (26). Since each size range is represented by six droplets of different initial angular position, the factor of 1/6 occurs. The total mass flowrate of fuel is $\dot{m}_{fuel}$.

Results and Discussion.

The results of the statistical analysis of the angular variation of the flow parameters is presented in Figs. 4(a) to 4(e). Percentage standard deviations are given for J values of 3, 9 and 16 as indicated in the key (Fig. 4(f)). It can be seen that angular variation of all five parameters is generally less than 20% upstream of the primary air injection, at which point it begins to increase very rapidly. It would therefore appear that in the region downstream of the grid location at which I is equal to 10 the flow field can be considered to be three-dimensional and to be two-dimensional upstream from this point.

The results of calculations for fuel sprays of evaporating droplets are shown graphically in Figures 5 to 9 as follows:-

	included cone angle (degrees)	spray velocity (m/s)
Fig. 5	45	20
Fig. 6	45	10
Fig. 7	45	50
Fig. 8	30	20
Fig. 9	80	20

Distance from atomiser nozzle to sheet break-up is taken as 5mm. The number of size ranges is 20 except for Fig. 8 where it was reduced to 12 to reduce the amount of computer time required. Other relevant data can be found in the programme listing of Appendix 1.

The results are shown as an orthographic projection of the droplet trajectories consisting of a side elevation of the combustor and an end elevation looking along the axis of the combustion chamber. The air injection locations are indicated by arrows. Droplet burn-out locations are encircled. Droplets whose loci do not end in a circle have hit the combustor wall.

The combustor dimensions are shown in Fig. 1. Part of the section of the combustor can downstream of the primary air injection holes is not shown in Figs. 5 to 9 .

Figure 5 shows the predicted spray obtained for an included nominal cone angle of 45° and initial spray velocity of 20 m/s, these characteristics being typical of the pressure-jet type of atomiser. It can be seen that a large number of droplets penetrate into the three-dimensional region. Those droplets passing within the vicinity of the primary air stream are deflected and some pass right across the combustion chamber and impinge on the opposite wall. Similar behaviour is observed in Fig. 6 where the spray velocity is only 10 m/s , as a result of which the droplets have evaporated after travelling a shorter distance along the chamber. Figure 7 shows a higher velocity spray (50 m/s) which has resulted in a spray which remains in liquid form further along the combustion chamber, some droplets passing beyond the secondary air injection holes.

Figure 8 shows the behaviour of a spray with a narrower cone angle. The spray has been broken up to a greater extent than for the 45° cone angle because the majority of the droplets have entered the recirculation zone where there are greater velocity gradients. It can be seen that some droplets show an apparently erratic behaviour as they are repeatedly deflected by several primary and secondary air streams.

Figure 9 shows a spray with a large cone angle (80°). In this case no droplets have penetrated into the three-dimensional zone and a large proportion of the droplets have collided with the combustor wall upstream of the primary air injection holes.

Figure 10 is a histogram showing the mass flow rate of fuel (area on graph) against distance along the x-axis of the combustor. This has been calculated for the 30° cone angle case of Fig. 8. It shows that a significant proportion of the fuel evaporates in the three-dimensional region of the combustor can.

In view of the fact that some droplets show a very abrupt deviation from their original path in the vicinity of the air injection streams, a check was considered necessary to ensure that this was not due to inaccuracies in the solution procedure arising from too large a time step length. The time step length was therefore reduced by a factor of four, and several sets of trajectory calculations were performed to verify the original results. There was no significant change in the results.

Conclusions.

It has been demonstrated that, according to the computer-predicted flow data, the conditions in the region of the primary air injection holes and downstream from this point are three-dimensional in nature. It has also been shown that it is possible to produce a three-dimensional mathematical model of individual droplet trajectories within a fuel spray and thus to model the spray as a whole. In the absence of any experimental data it has not been possible to perform a comparison between the predicted and actual observed spray behaviour. Experimental data to verify the predictions is still required.

It can be seen, however, that the techniques developed could be of use in combustor design. It is clearly undesirable to have droplets impinging on combustor walls causing 'wet' spots, or to have un-evaporated fuel surviving as far as the lower temperature regions of the combustor where it may lead to incomplete combustion and consequently poor fuel efficiency and the presence of pollutants in the exhaust gases. The effect of cone angle and spray velocity on these phenomena has been shown. Further study along these lines might enable a more suitable atomiser design to be found or lead to improvements in combustion chamber design with particular regard to the positioning of the air injection ports.

It must be noted that although the droplet/particle trajectory algorithm has been applied to the specific case of evaporating droplets in gas turbine combustors, it remains a general procedure and is capable of being used to model the motion of any particle or droplet in a three-dimensional flow field. Examples of applications include diesel engines and cyclone separators.

References.

1) Swithenbank, J., Turan, A., Felton, P. G., and Spalding, D.B. 'Fundamental Modelling of Mixing, Evaporation and Kinetics in Gas Turbine Combustors.' September, 1979. (HIC 320)

2) Turan, A. 'A Three-Dimensional Model for Gas Turbine Combustors'. September, 1978. (HIC 298).Univ. of Sheffield Ph.D. Thesis.

3) Dickerson and Schumann. Journal of Spacecraft: 2, 99, 1956.

4) Wise, H., and Agoston, G. A. 'Literature on the Combustion of Petroleum', American Chemical Society, Washington D.C., 1958.

5) Boyson, F., and Swithenbank, J. 'Spray Evaporation in Recirculating Flow'. Colloqium on Turbulent-Combustion Interactions. 1978.

6) Williams, A. 'Combustion of Sprays of Liquid Fuels' Elek Science, London 1976.

7) Vincent, M. W. 'Fuel Spray Evaporation in Gas Turbine Burners' University of Sheffield Ph.D. Thesis. July, 1973.

8) Clift, R., Grace, J. R., Weber, M.E. 'Bubbles, Drops and Particles'. Academic Press, 1978.

List of Figures.

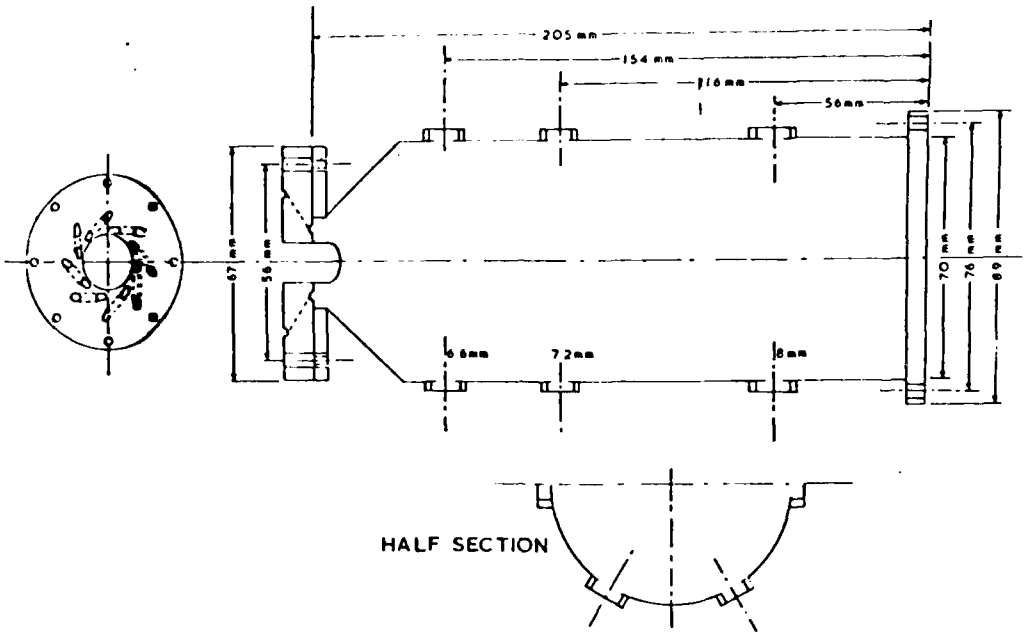

Figure 1 : Geometry of Lycoming combustor can.

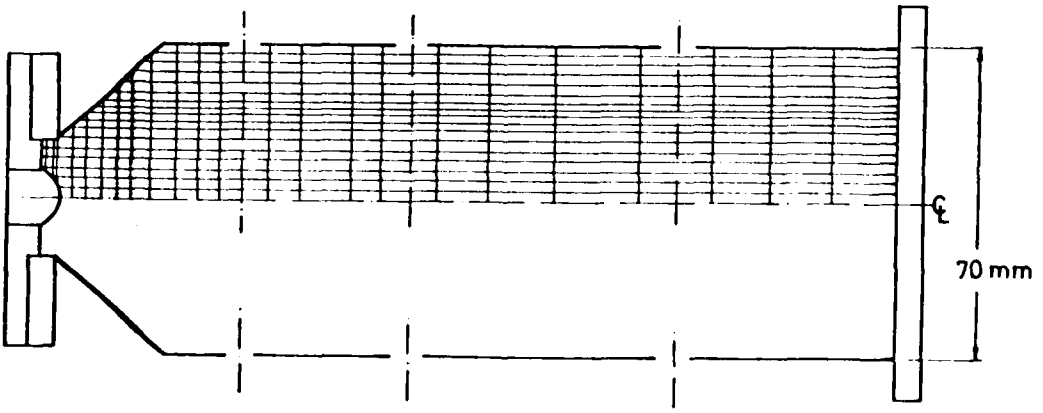

LYCOMING COMBUSTOR,
GRID ARRANGEMENT 27 x 18 x 7 = 3 402 TOTAL POINTS

Figure 2 : Finite difference grid for the Lycoming combustor.

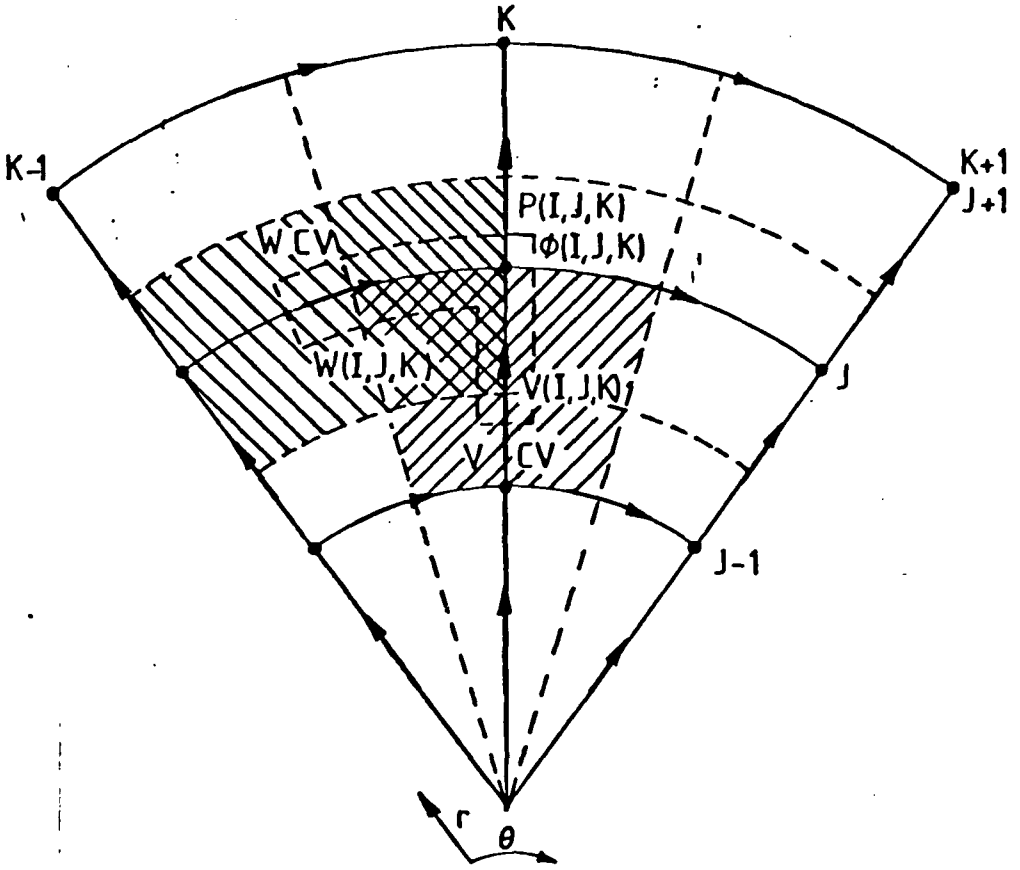

W- AND V-VELOCITY CONTROL VOLUMES IN r-θ DIRECTIONS.

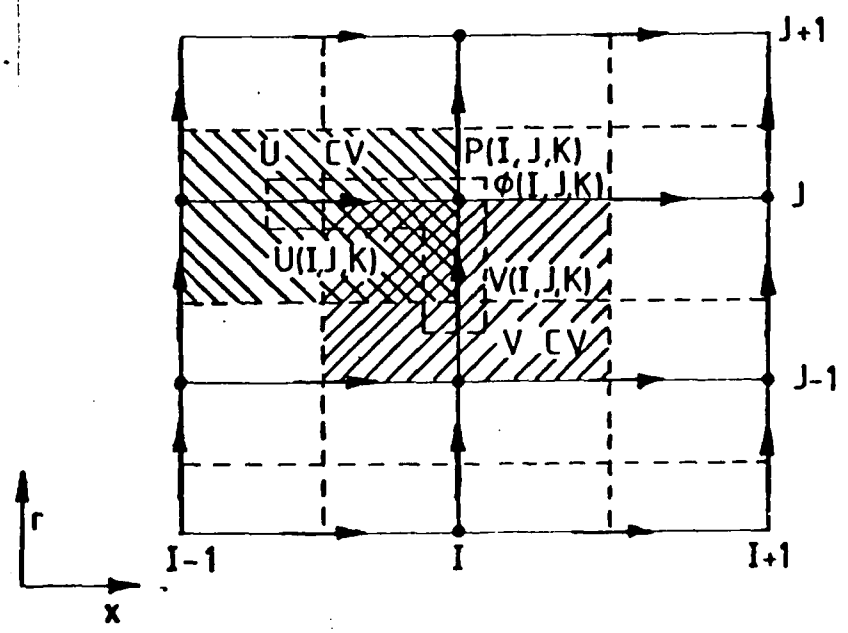

U-AND V-VELOCITY CONTROL VOLUMES IN r-x DIRECTIONS.

Figure 3(a) : Location of u-, v- and w-velocity control volumes.

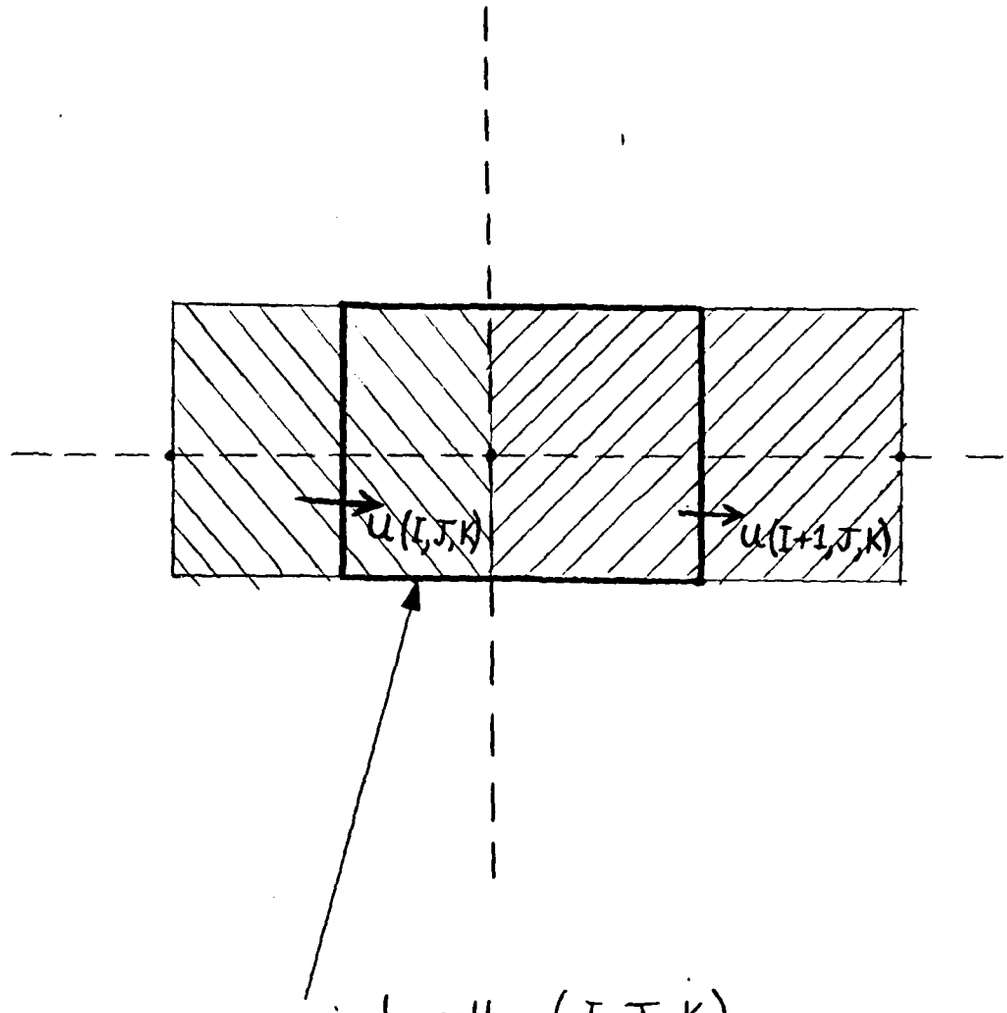

$$u = \frac{u(I,J,K) + u(I+1,J,K)}{2}$$

Figure 3(b) : Relocation of u-velocity control volumes.

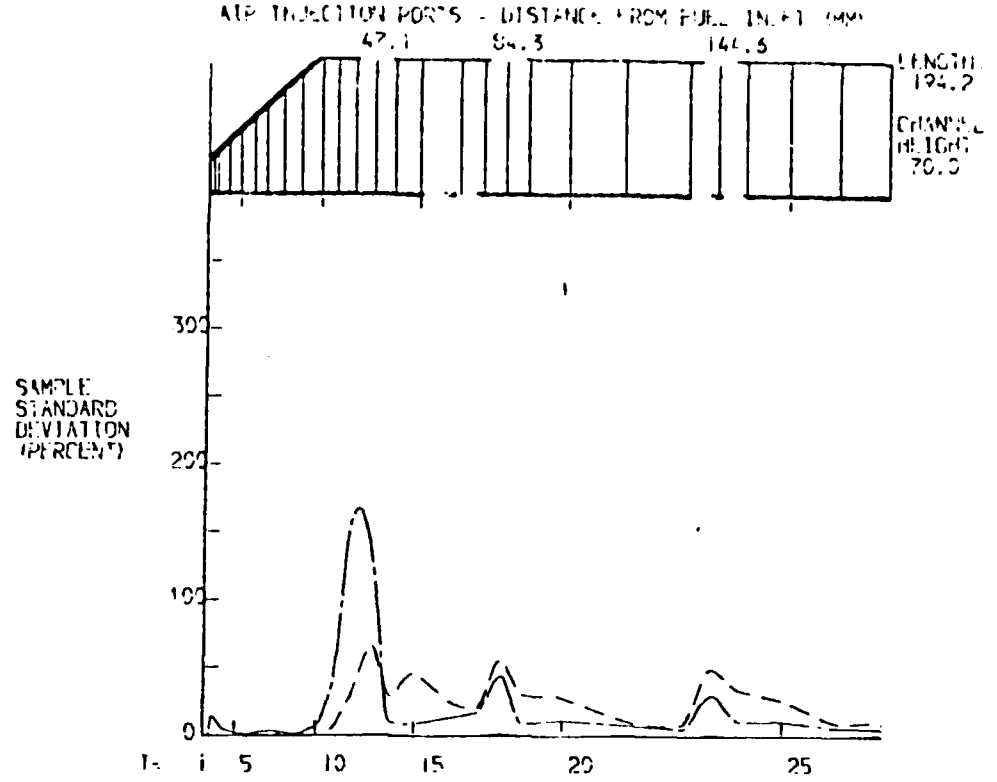

FIGURE 4(a) ANGULAR VARIATION OF U-VELOCITY

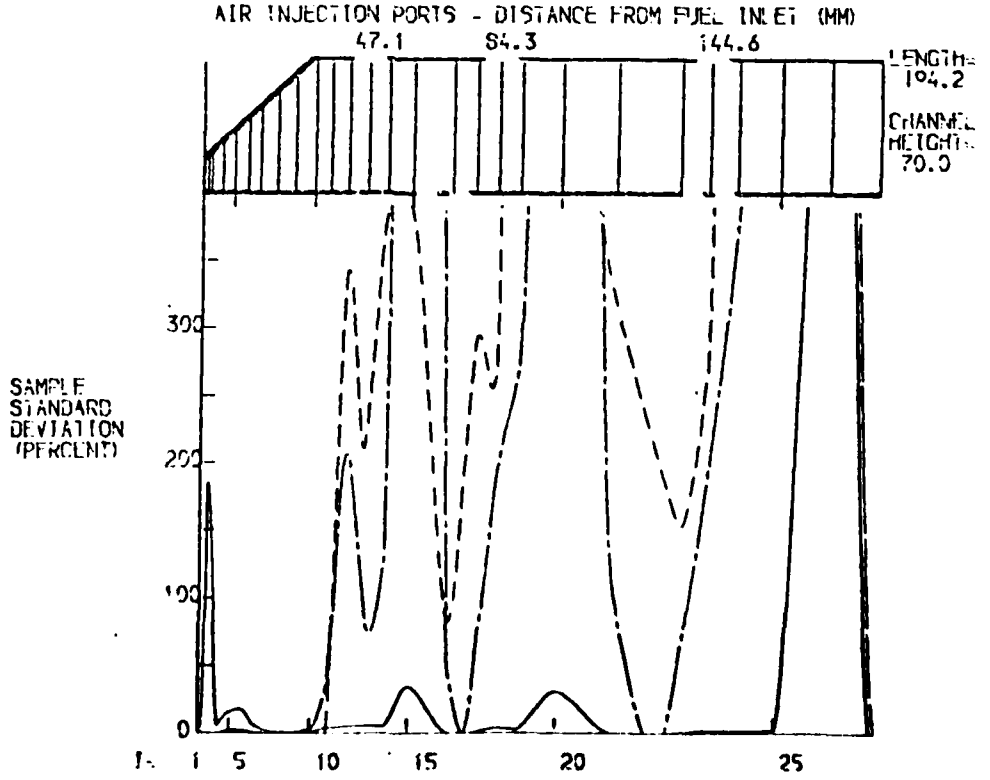

FIGURE 4(b) ANGULAR VARIATION OF V-VELOCITY

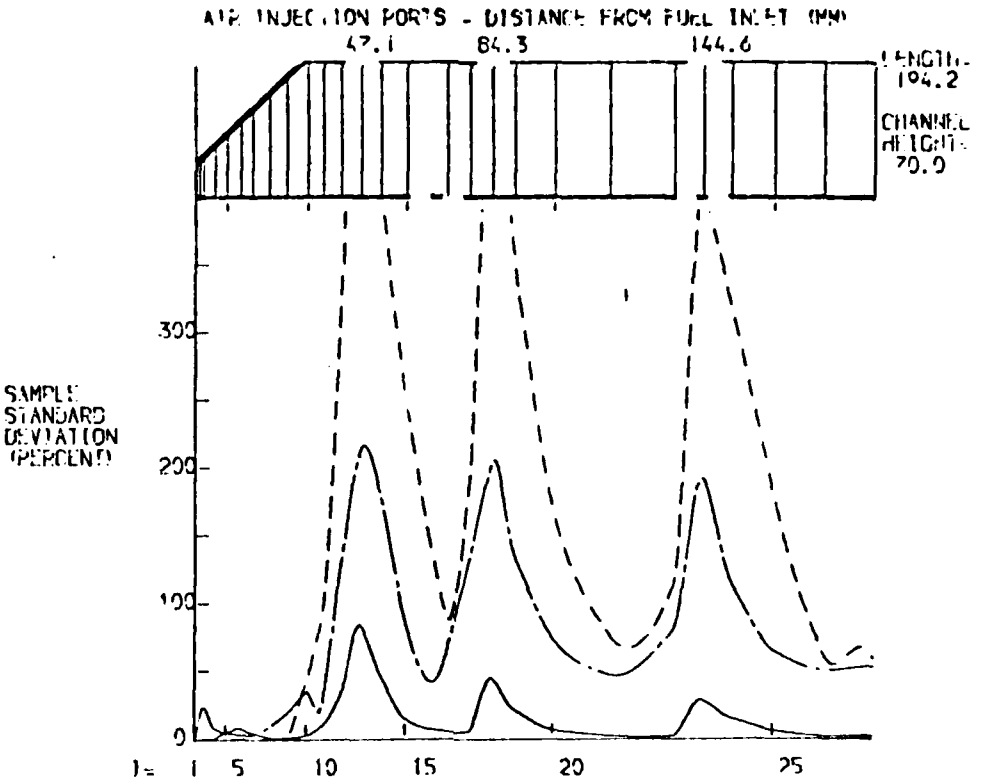

FIGURE 4(c) ANGULAR VARIATION OF W-VELOCITY

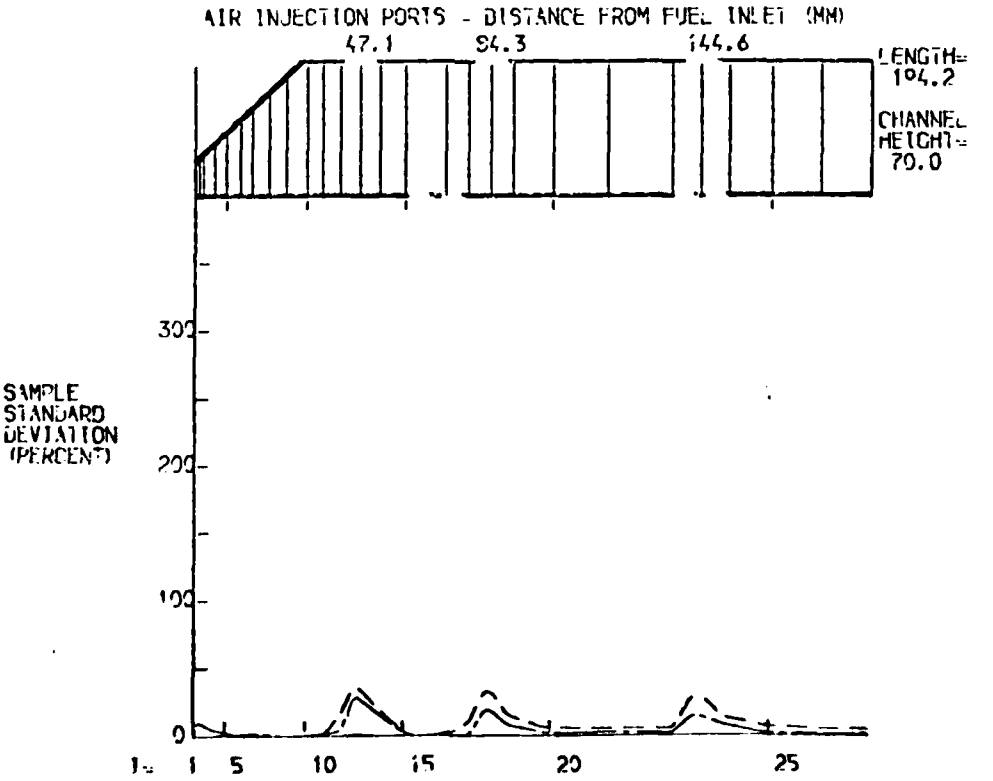

FIGURE 4(d) ANGULAR VARIATION OF TEMPERATURE

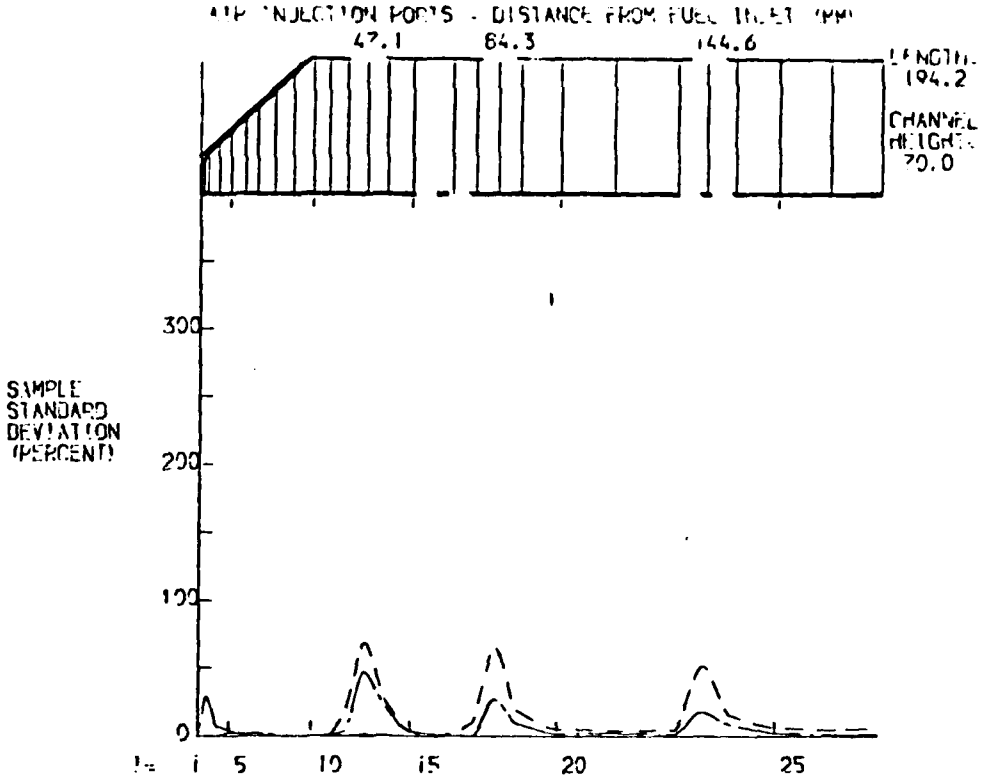

FIGURE 4(e) ANGULAR VARIATION OF DENSITY

KEY

J=3 ————————

J=9 —·—·—·—·—

J=16 - - - - - - - - - -

FIGURE 4(f)

Figure 4(g).

VELOCITY FIELD .POSITION K = 4

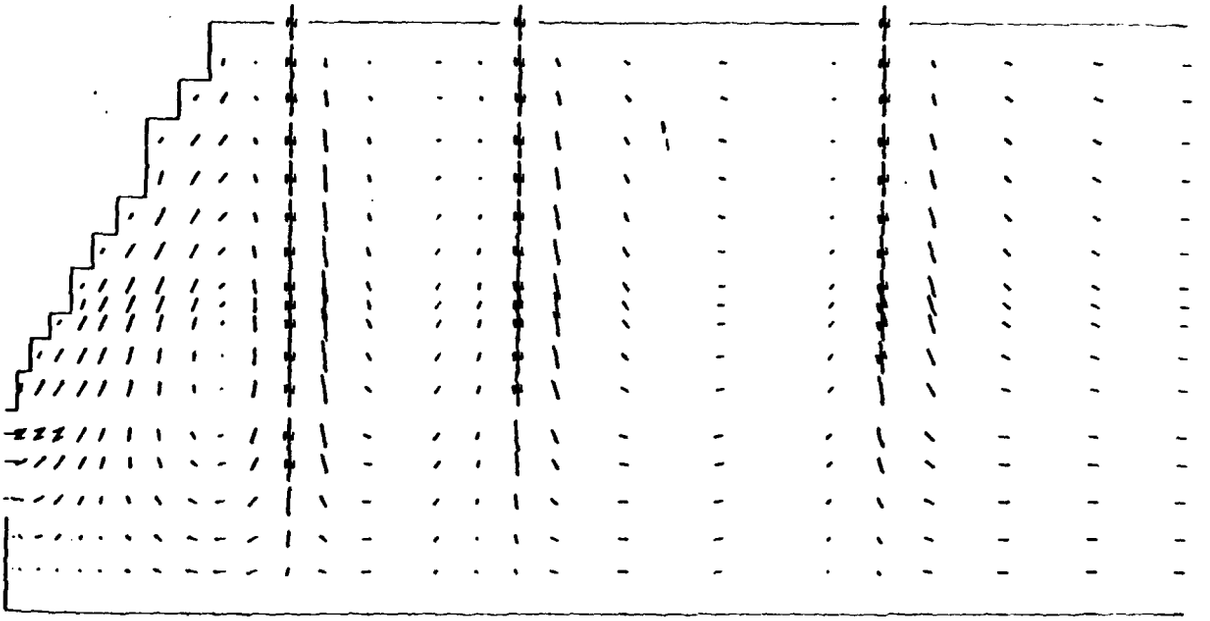

Figure 4(h) : VELOCITY FIELD .POSITION I = 13

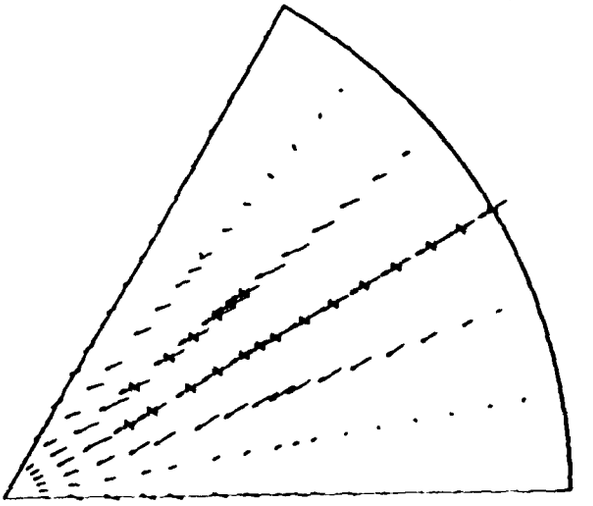

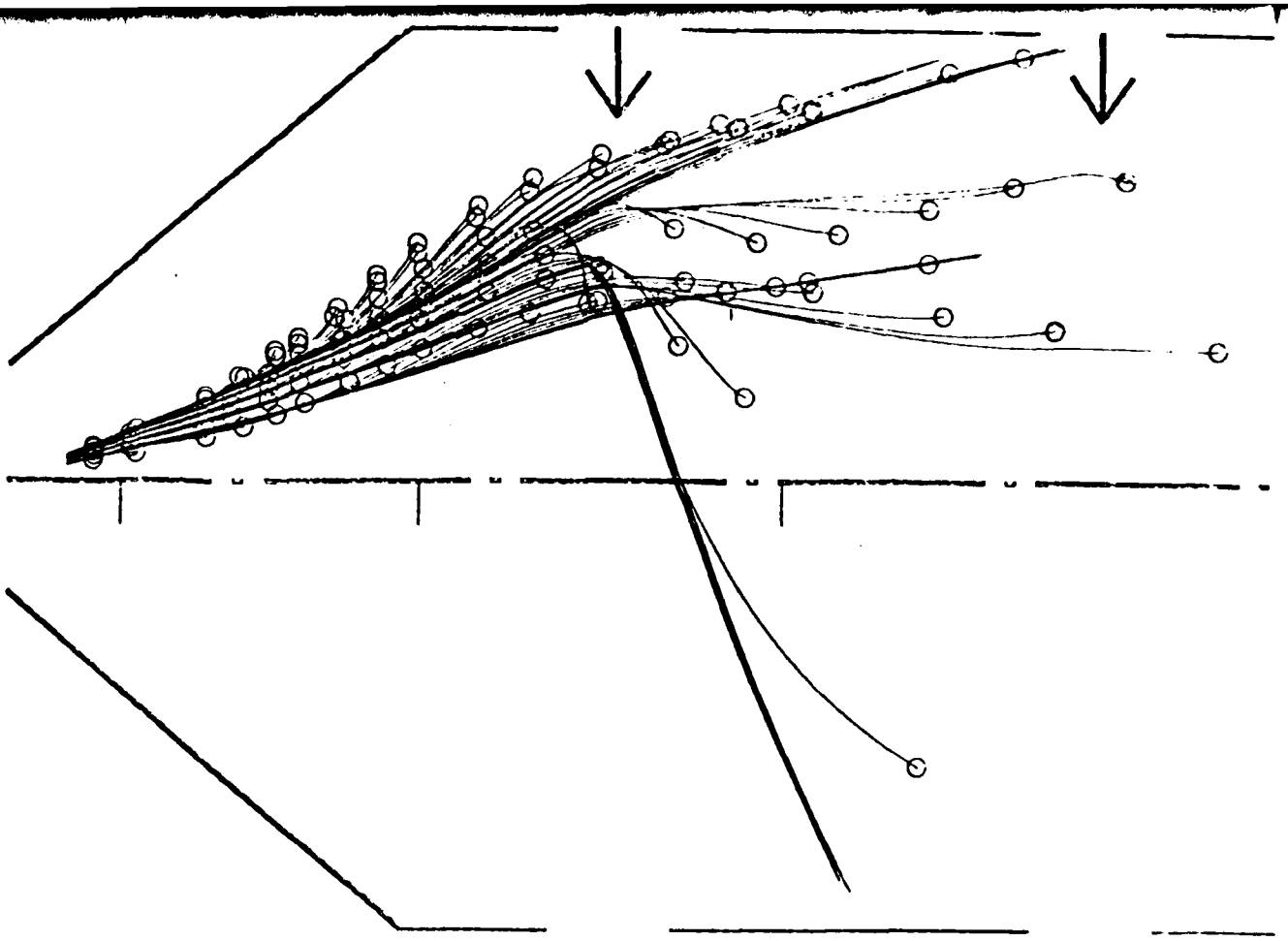

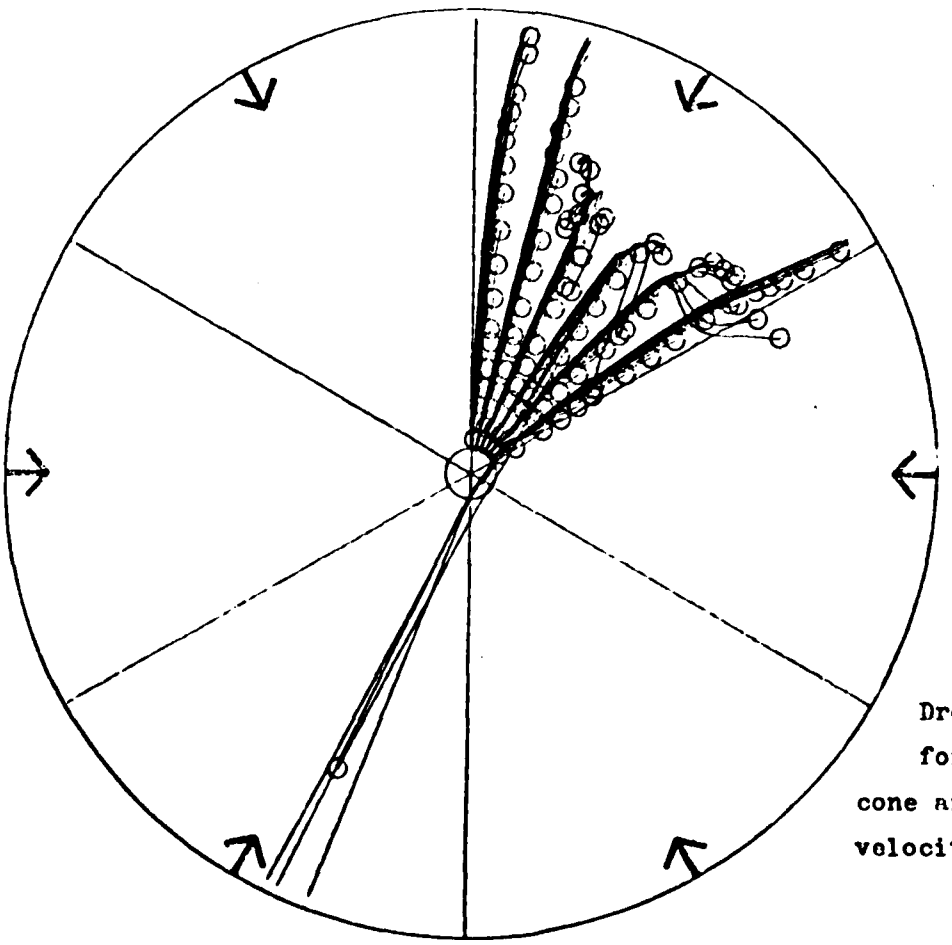

FIGURE 5
Droplet trajectories
for Spray:
cone angle = 45°
velocity = 20 m/s

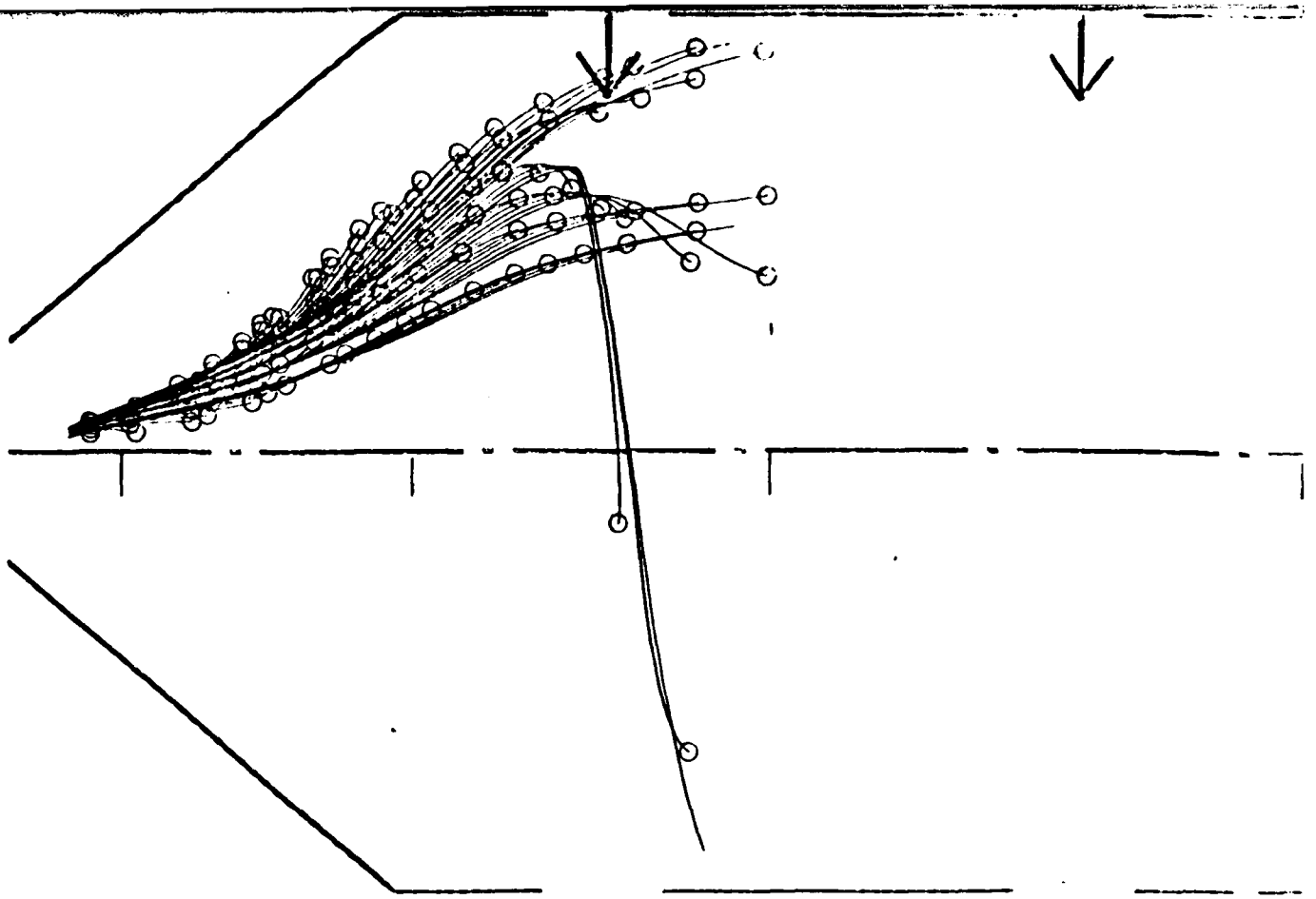

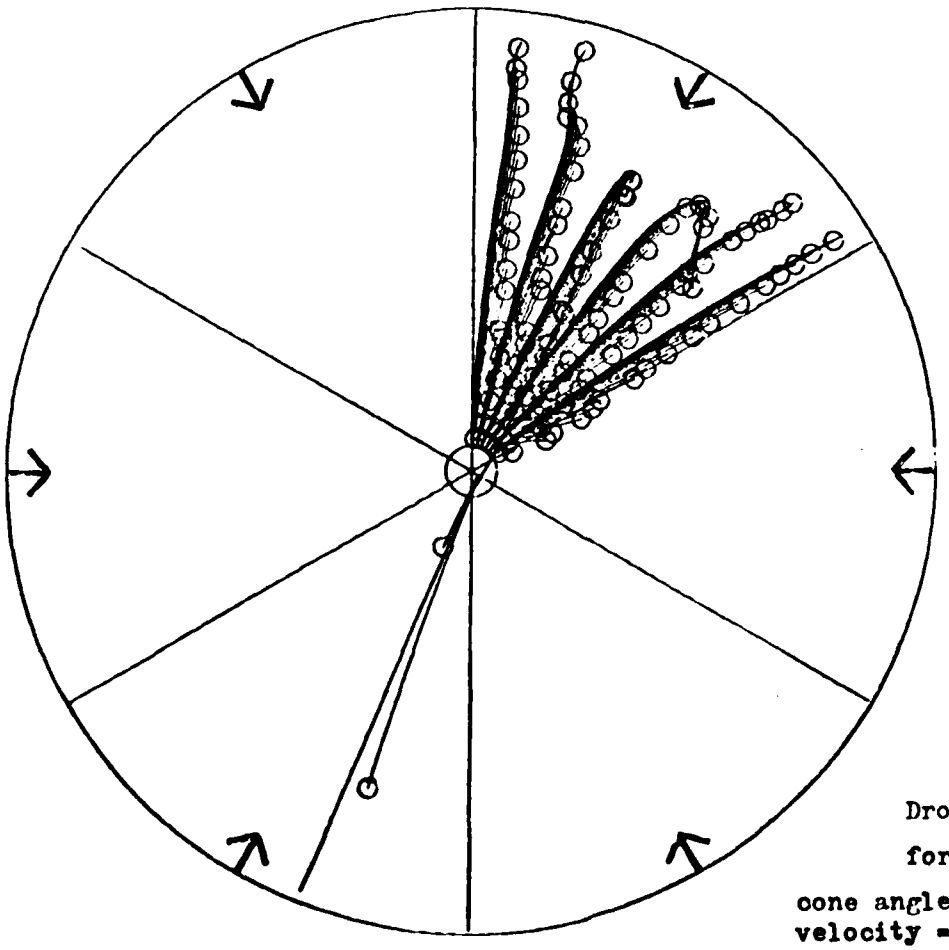

FIGURE 6

Droplet trajectories

for Spray:

cone angle = 45°

velocity = 10 m/s

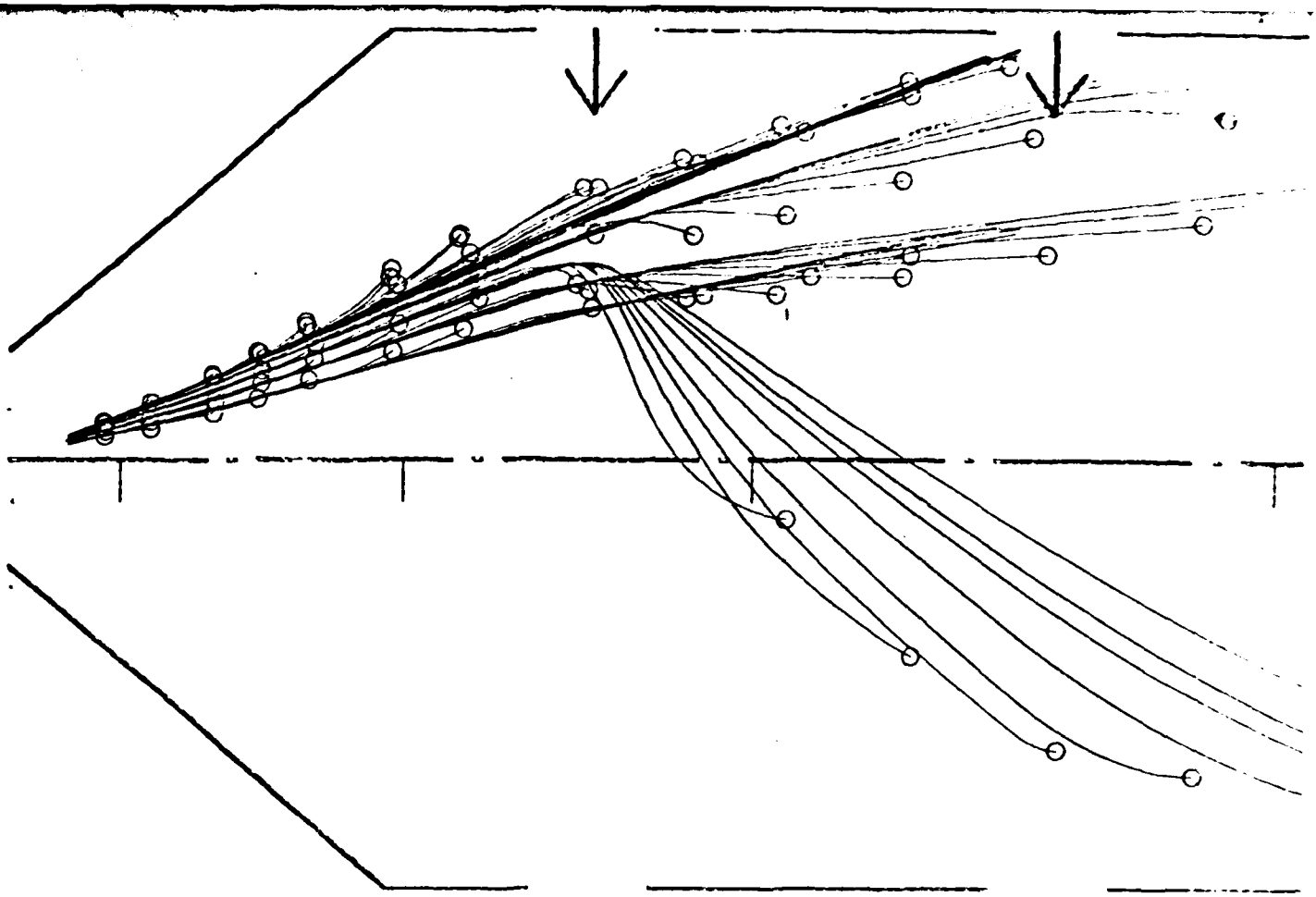

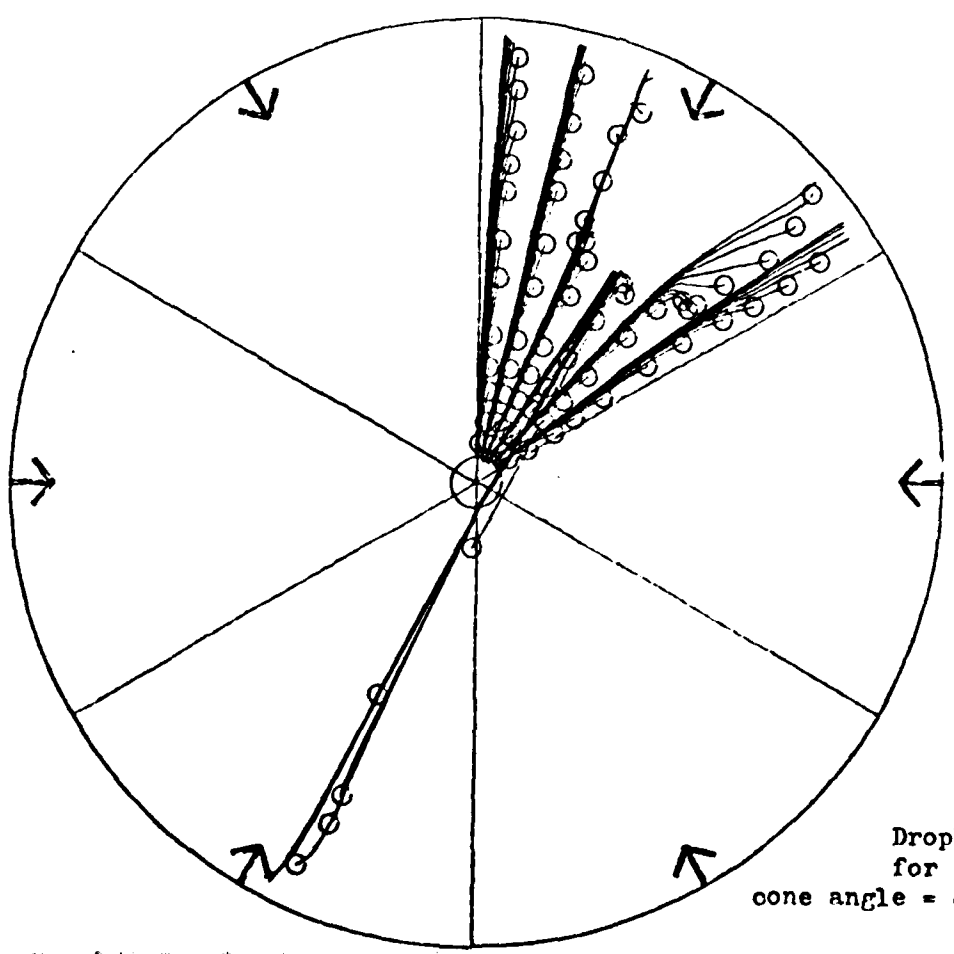

FIGURE 7

Droplet trajectories
for Spray :
cone angle = 45°, velocity = 50 m/s.

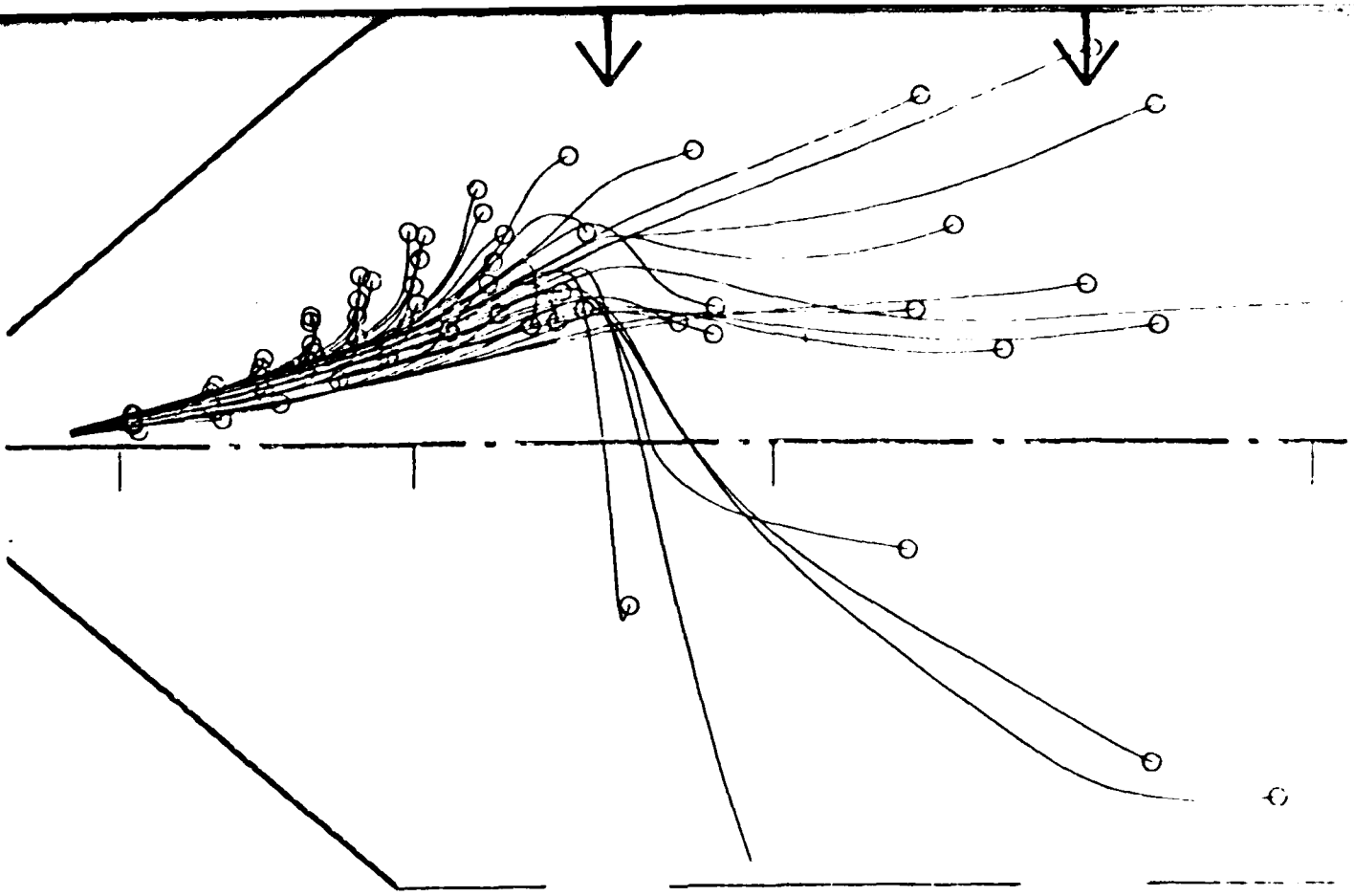

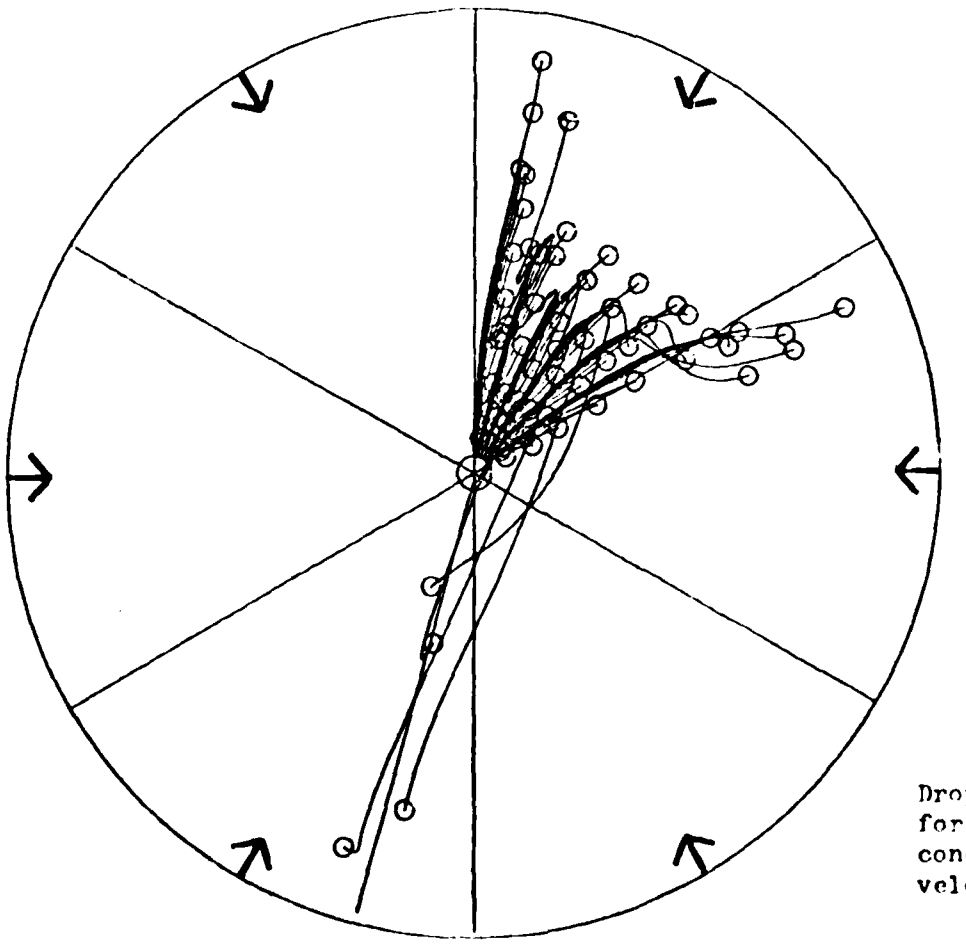

FIGURE 8

Droplet trajectories
for Spray :
cone angle = 30°
velocity = 20 m/s.

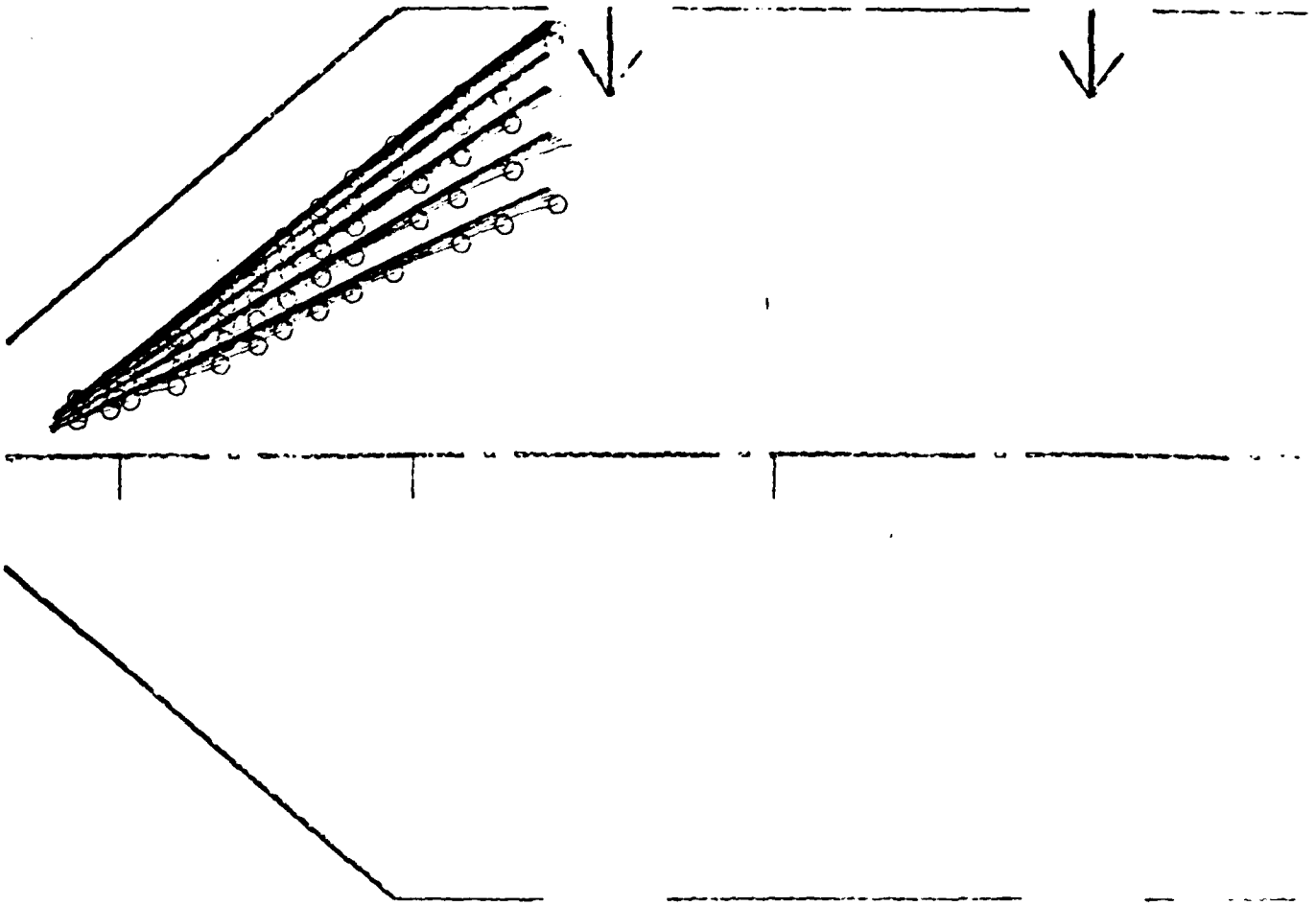

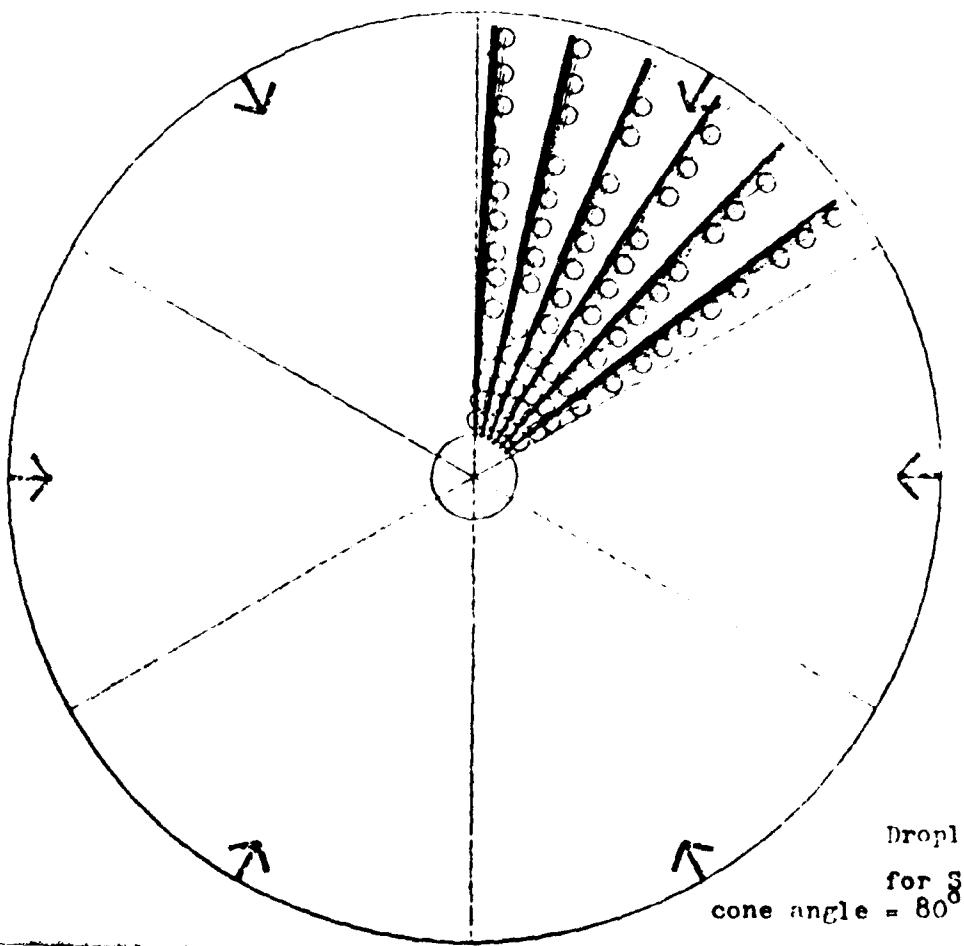

FIGURE 9

Droplet trajectories

for Spray :

cone angle = 80°, velocity = 20 m/s.

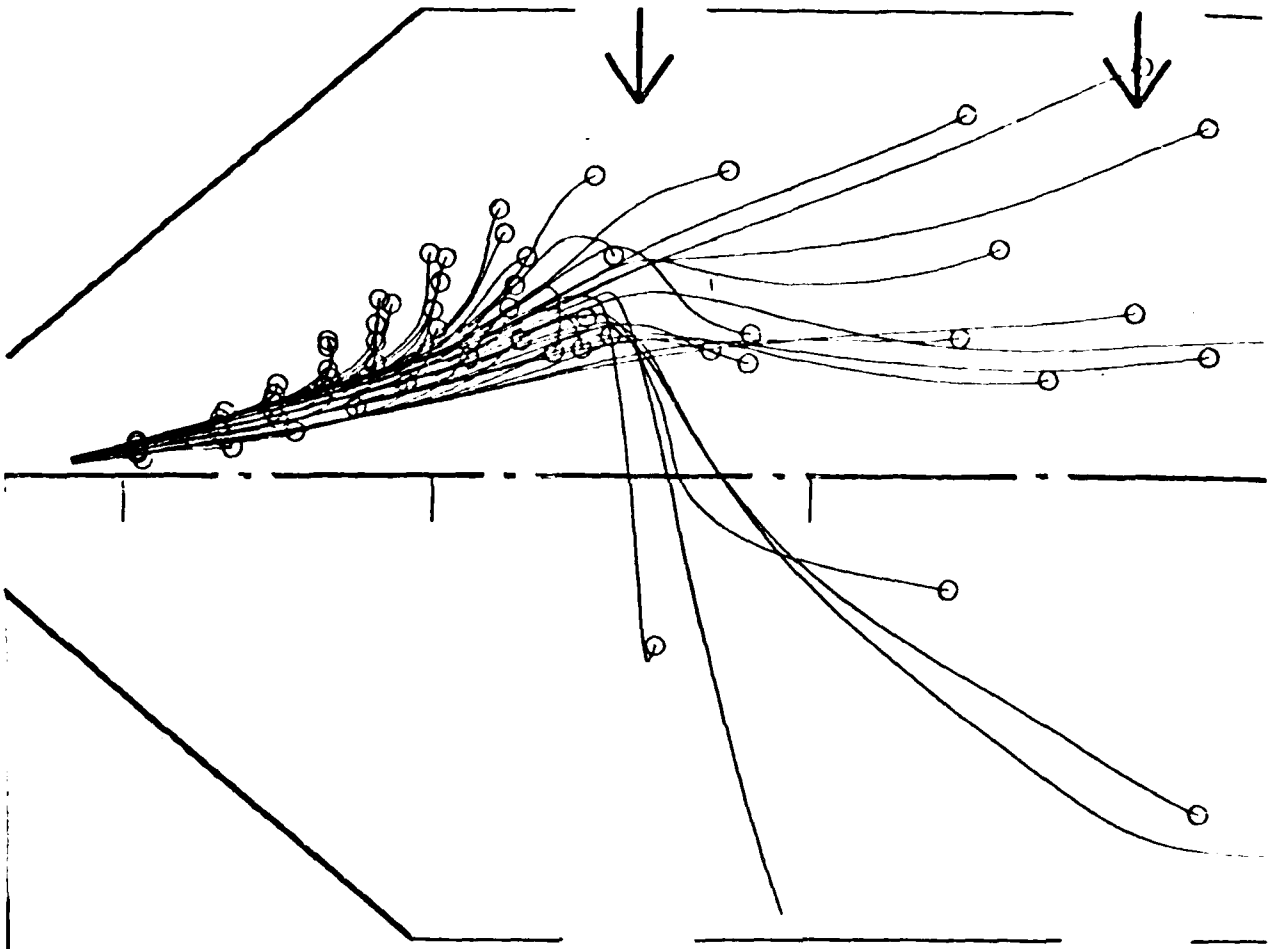

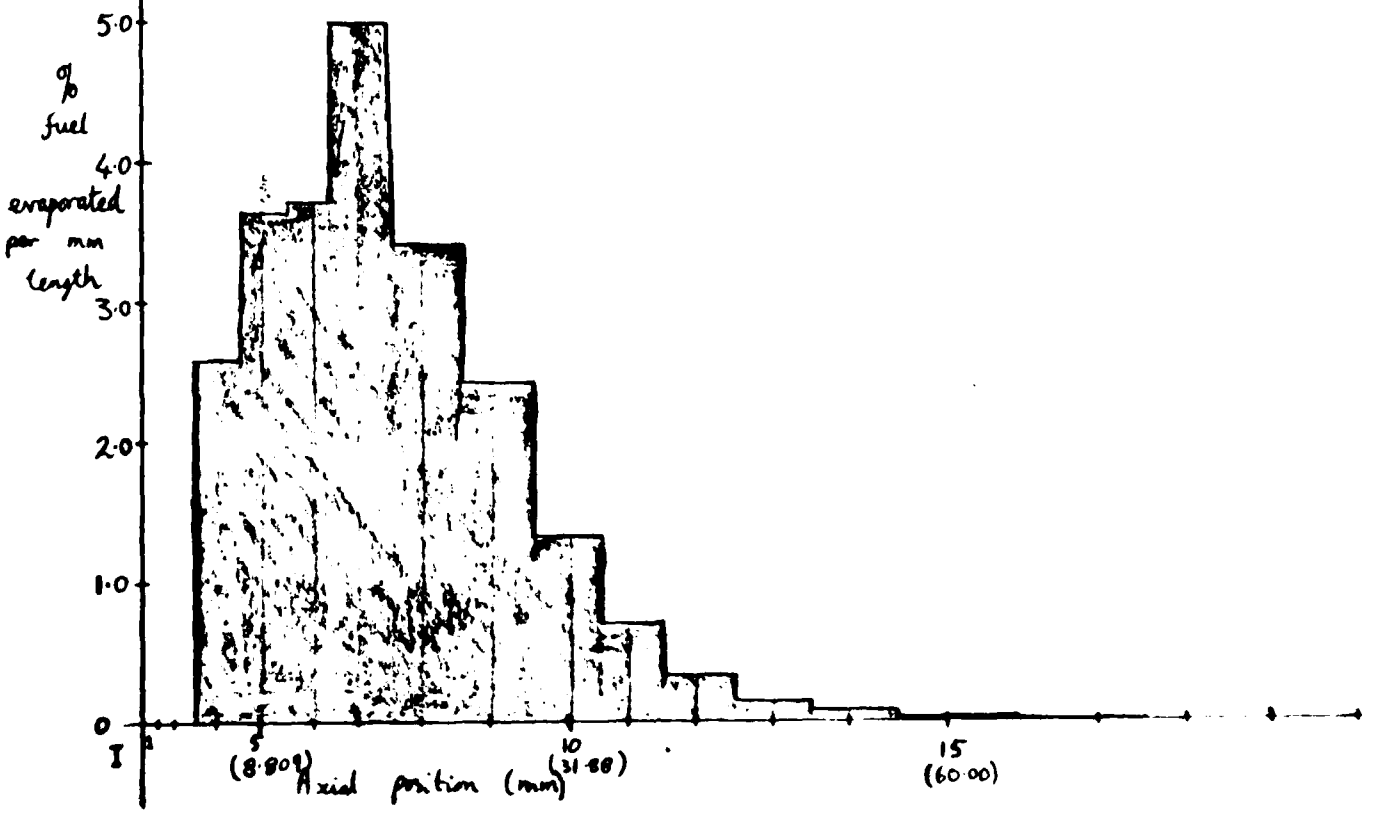

Figure 10: Histogram of mass flow-rate of fuel vapour vs. distance along X-axis.